

# Performance Enhancement of Polycrystalline Silicon Solar Cell through Sputter Coated Molybdenum Disulphide Surface Films

Prashanth SHANMUGAM<sup>1</sup>, Rajasekar RATHANASAMY<sup>2,\*</sup>,  
Gobinath VELU KALIYANNAN<sup>3</sup>, Santhosh SIVARAJ<sup>2</sup>, Moganapriya CHINNASAMY<sup>2</sup>,  
Manju Sri ANBUPALANI<sup>4</sup>

<sup>1</sup> Department of Aeronautical Engineering, Excel Engineering College, Namakkal, Tamil Nadu, 637303, India

<sup>2</sup> Department of Mechanical Engineering, Kongu Engineering College, Perundurai, Tamil Nadu, 638060, India

<sup>3</sup> Department of Mechatronics Engineering, Kongu Engineering College, Perundurai, Tamil Nadu, 638060, India

<sup>4</sup> Department of Chemical Engineering, Kongu Engineering College, Perundurai, Tamil Nadu, 638060, India

**crossref** <http://dx.doi.org/10.5755/j02.ms.29364>

Received 30 June 2021; accepted 09 September 2021

The current research focuses on sol-gel derived synthesis and RF sputter deposition of molybdenum disulphide (MoS<sub>2</sub>) over polycrystalline Si solar cell. Various coating layers were obtained under different sputter deposition at regular intervals. The influence of MoS<sub>2</sub> sputter coating on optical, thermal chemical structural properties was examined through various characterisation techniques. 30 minutes coated solar cell reported maximum light transmittance of 95 % in the visible spectrum and minimum electrical resistivity of  $2 \times 10^{-3}$  ohm-cm. 30 minutes coated solar cell exhibited maximum power conversion efficiency (PCE) of 19.19 % (open source) and 21.01 % (controlled source). Thermal imaging data reveal that the optimal coating layer experiences a minimum temperature of 33.9 °C and 49.9 °C. From experimental results, sputter deposited MoS<sub>2</sub> Si solar cells experience minimum light reflectance and enhanced cell performance.

**Keywords:** molybdenum disulphide, sputter coating, anti-reflection coating, power conversion efficiency, polycrystalline silicon solar cell.

## 1. INTRODUCTION

Clean and green energy is quite necessary as it emits zero percent carbon dioxide to overcome global warming and the greenhouse effect [1]. Some of the unconventional renewable energy sources are geothermal energy, hydel energy, tidal energy, wind energy, solar energy, etc.. Among those energies, solar energy is available abundant in nature and capable of satisfying future energy needs [2]. In recent years, many researchers were focussing on the performance enhancement of solar cells. This lead to the generation of electrical energy at a very cheap rate as compared to conventional energy resources. Silicon based photovoltaic cells were categorised broadly into two categories: monocrystalline and multicrystalline solar cells [3]. Monocrystalline solar cells are fabricated from the single source of Si and often appear black in colour. Whereas polycrystalline Si solar cell was fabricated from various sources of Si and hence their manufacturing cost is low as compared to a monocrystalline solar cell. Hence polycrystalline Si solar cells were commercially successful in the solar cell market. Initially, the sunlight incident at a certain angle over the solar cell surface. The incident light is then transmitted into the protective layer and reaches the depletion region. Then the energy of incident photon is higher than the energy band gap of the photoactive layer. A certain part of incident light gets reflected at the surface of the solar cell. By utilising the reflected light, the power conversion efficiency (PCE) of solar cell can be improved easily [4]. The antireflective coating (ARC) is the only way

to reduce the reflection of light at the cell surface [5]. This in turn increases short circuit current ( $I_{sc}$ ) and open circuit voltage ( $V_{oc}$ ).

Some of the ARC materials which are coated through various methods are TiO<sub>2</sub>, SiO<sub>2</sub>, zirconia, monazite, CaTiO<sub>3</sub>, SrTiO<sub>3</sub>, MoSe<sub>2</sub>, ZnAl<sub>2</sub>O<sub>4</sub> etc. Materials with huge light trapping ability can be used as antireflective coatings [6–9]. Transition metal dichalcogenide MoS<sub>2</sub> is recognized as effective antireflective material in the visible light spectrum. The energy band gap of MoS<sub>2</sub> is found to be 1.8 eV [10]. Thin film ARC can be deposited over solar cell surface through various techniques such as slot-die coating [11], blade coating [12], spin coating [13], sputter coating [4], electrospinning [14, 15], spray pyrolysis [16] etc.

This current research work focuses on the synthesis and deposition of MoS<sub>2</sub> nanolayer over the solar cell surface. The ARC material is deposited through the radio frequency (RF) sputter deposition technique for attaining enhanced light transmittance. The coated solar cell was analysed under direct sun (open source) and neodymium illumination (closed source). The optical, electrical, thermal, structural, chemical, and morphological studies of MoS<sub>2</sub> deposited nano-layers can be examined through different characteristic techniques.

## 2. EXPERIMENTAL TECHNIQUES

The chemical required for the synthesis and deposition of MoS<sub>2</sub> were purchased with a high purity level at Sigma Aldrich. The solar cell indulged in the process of

\*Corresponding author. Tel.: +91 9952460698.

E-mail address: [rajamech@kongu.ac.in](mailto:rajamech@kongu.ac.in) (R. Rathanasamy)

performance enhancement was a commercial polycrystalline Si solar cell. The standard solar cell with dimensions 5.2 cm × 3.8 cm was procured from Vikram Solar, India.

## 2.1. Synthesis of molybdenum disulphide

For the synthesis of transition metal dichalcogenide MoS<sub>2</sub>, first and foremost 0.2 grams of ammonium molybdate tetrahydrate was dissolved in 800 ml of deionized water. Then 400 mg of thioacetamide was added with the existing mixture and then stirred at a constant rate. Followed by the addition of 50 mg of diethylenetriamine pentaacetic acid and then stirred for about 120 minutes for attaining brown sol. The brown sol is dried in a hot air oven at 65 °C for 13 hours resulting in the formation of a bronze coloured gel. Thus, obtained xerogel is placed in a tube furnace under argon atmosphere at 180 sccm lead to the formation of MoS<sub>2</sub>.

## 2.2. Pelletisation and sputter deposition of MoS<sub>2</sub>

The material which is to be sputter coated over the surface should be in solid circular disc form with the approximate dimension of 5 cm diameter and 0.48 cm thickness. The target was initially loaded into the mild steel die containing base plate, solid and hollow shaft like arrangement. With the help of the universal testing machine, a very high compressive force of 1.35 GPa was imposed on mild steel die resulting in the formation of the solid target material.

The silicon solar cell was initially pre-cleaned with ethanol and dried for 5 minutes at room temperature. Then the solar cell and the prepared solid target were loaded in the substrate and target holder. The reactor used in the deposition process is RF magnetron sputtering reactor[17]. Sputter power of 250 W was supplied to the target material which is a place at the argon atmosphere. The generated plasma ionises the argon gas. Now, the ionised argon gas sputters off the target material elements and thus facilitates thin deposition over the substrate. The sputter deposition of MoS<sub>2</sub> was performed under various sputtering time such as 10, 20, 30, and 40 minutes. The various MoS<sub>2</sub> coated samples were represented as M1 (10 min), M2 (20 min), M3 (30 min), and M4 (40 min). These layers were deposited at a vacuum pressure of 6 N/m<sup>2</sup>. The operating parameters of sputter deposited MoS<sub>2</sub> are shown in Table 1.

**Table 1.** Operating parameters of sputter deposited MoS<sub>2</sub>

Deposition layers	Time duration, mins	Layer thickness, nm	Substrate target distance, cm	Sputter Power, W
M1	10	98	4.5	250
M2	20	176		
M3	30	288		
M4	40	378		

## 2.3. Characterization methods

The structural properties and crystallinity level of synthesised MoS<sub>2</sub> were examined through X-ray diffraction technique on X'Pert Proanalyzer. The surface of various MoS<sub>2</sub> coated samples, in addition to their coating thickness,

were analyzed through FE- SEM technique using TESCAN MIRA 3. The chemical constitution of optimal thin film sputter coating was found using energy dispersive spectroscopy (EDAX). Then surface morphology of optimal thin film coating in 2D and 3D was determined through atomic force microscopy (AFM) using Tosca 400. The optical properties such as transmittance and reflectance were interpreted under the open and closed atmospheric conditions with the help of UV- visible spectroscopy on Varian Cary 5000. I-V characteristic curves of the various coated samples under open and closed conditions were obtained using Keithley 2450 source meter. The electrical resistivity of solar cell samples has been examined through the four probe technique on Four probe SK012. The effect of temperature on different coated samples was studied using IR Fluke thermal imager.

## 3. RESULTS AND DISCUSSION

The diffraction peaks of synthesized transition metal dichalcogenide match exactly with the standard JCPDS card No. 00-037-1492 and confirms the cubic crystal arrangement. The peaks of diffraction were found to be sharp. The sharp diffraction peaks indirectly represent the high crystalline nature of synthesised MoS<sub>2</sub> powder. The Miller indices of synthesised ARC material was interpreted as follows: (002), (100), (101), (102), (103), (106), (105), (106), (110), (008) and (108). The XRD diffraction peak positions were indicated in Fig. 1.

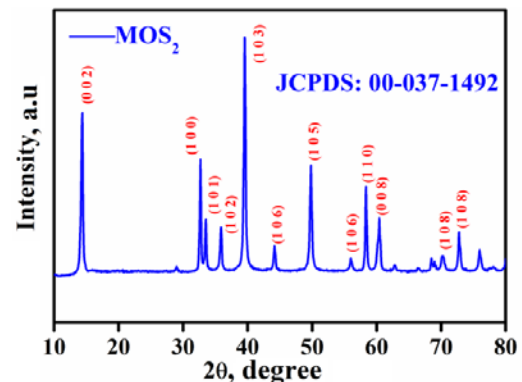
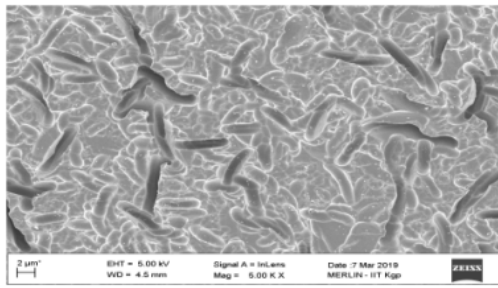


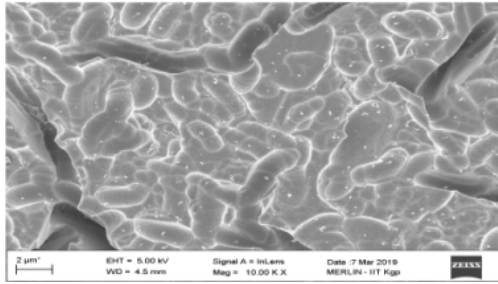
**Fig. 1.** XRD pattern of synthesised MoS<sub>2</sub>

The surface morphology of various thin film MoS<sub>2</sub> coatings and their corresponding cross sectional thickness were studied using FESEM images and are indicated in Fig. 2 and Fig. 3. The compactness and dense surface coating were mainly based on different sputter deposition machining parameters such as sputter power, sputter time, vacuum chamber pressure, type of target material, the distance between target and substrate, sputter power, and type of inert gas used inside the chamber. The grains size increases until saturation state with the increase in sputter power and sputter time. The cross-sectional thickness of various sputter deposited MoS<sub>2</sub> silicon solar cells were found to be 98 nm, 176 nm, 288 nm, and 378 nm.

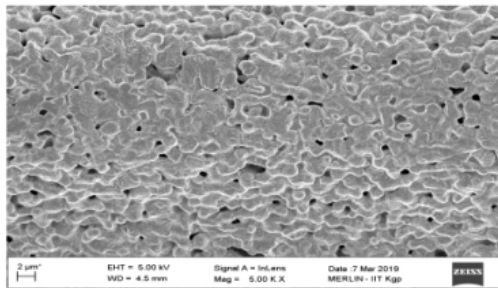
From these values, it is clear that increasing sputter coating time directly increases the thickness of the coating. The optimal coating thickness was found to be 288 nm at which maximum power conversion efficiency is achieved at both open and closed sources.



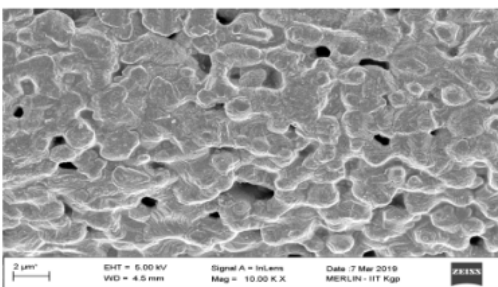
a



b



c



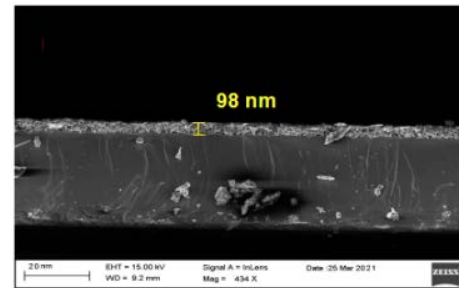
d

**Fig. 2.** Surface morphology of various ARC sputter coated solar cells through FESEM: a – M1; b – M2; c – M3; d – M4

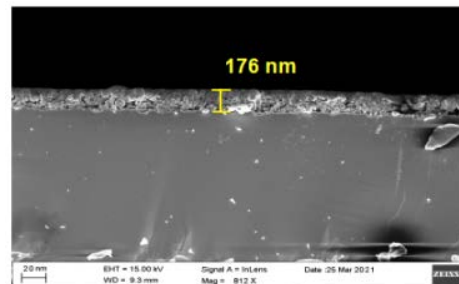
The elemental composition of optimal thin film MoS<sub>2</sub> coated solar cell (M3) was identified through energy dispersive X-ray spectrometer (EDAX) as shown in Fig. 4 and Table 2. The existence of elements such as S, Mo and Si at maximum amounts confirms the coated material as MoS<sub>2</sub>. The optimal solar cell (M3) was identified through the calculation of power output in response with the incident solar light.

**Table 2.** EDAX results of M3 coated solar cells

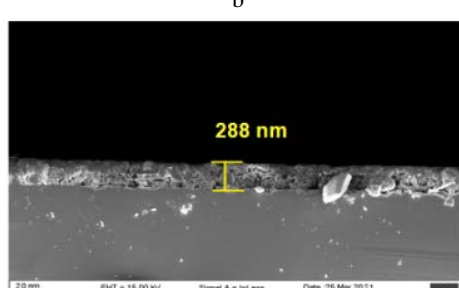
Element	Atomic percentage, %	Weight percentage, %	Net Int.
Si	87.8	63.1	838.96
Mo	4.66	18.2	92.67
S	3.24	17.13	36.02
Al	2.3	0.97	1749
Na	2.0	0.6	14.86



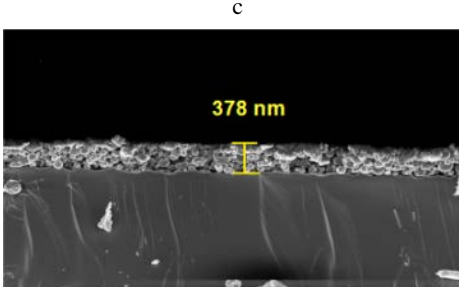
a



b



c



d

**Fig. 3.** Cross-sectional thickness of various ARC sputter coated solar cells through FESEM: a – M1; b – M2; c – M3; d – M4

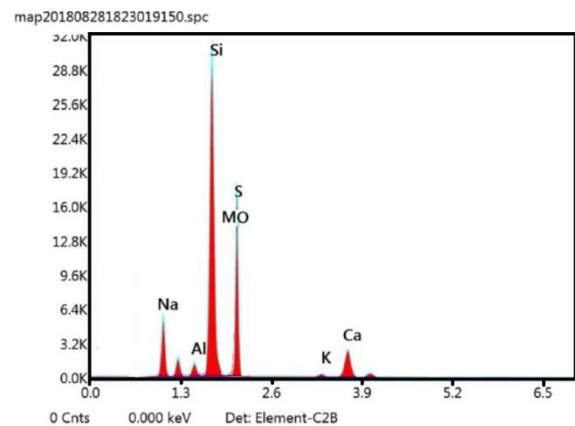


**Fig. 4.** EDAX spectrum of optimal coated solar cell (M3)

Through atomic force microscopy (AFM), the surface

topography of 30 minutes coated sample (M3) which exhibits maximum cell performance was evaluated. The RMS value of surface roughness within the approximated area of  $100 \times 10^{-12} \text{ m}^2$  was examined through tapping mode. The surface roughness values of various thin film coatings M1 to M4 coated samples were analysed through standard software and found to be 96, 82, 67 and 51 nm.

The two dimensional image and three dimensional view of optimal AR coated solar cell (M3) are shown in Fig. 5.

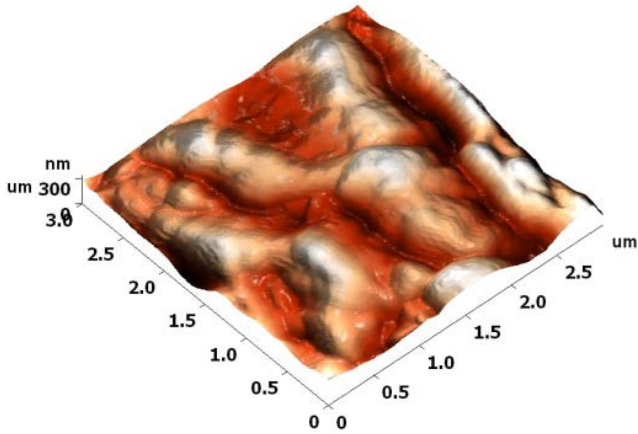


**Fig. 5.** 3D surface morphology of M3 coated solar cell through AFM technique

The  $\text{MoS}_2$  sputter coating in 30 minutes solar cell was found to be uniform to other surface coatings. The minimum surface roughness coated sample experiences minimum incident light scattering which in turn resulting in maximum light transmittance [2]. This paves the way for attaining maximum solar cell performance.  $\text{MoS}_2$  AR coatings on solar cell surface experience better light transmittance and minimal reflectance than uncoated solar cell in visible spectrum. The thin film coatings hold high degree of transparency. The light transmittance and reflectance of various coated solar cell and uncoated solar cell are plotted in Fig. 6 and Fig. 7.

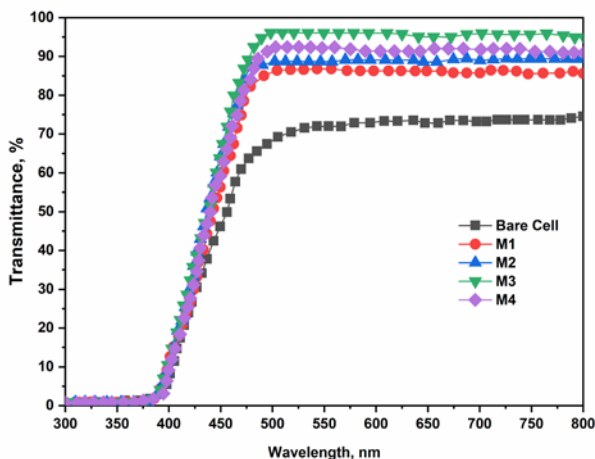


**Fig. 6.** Optical transmittance of various  $\text{MoS}_2$  sputter deposited solar cells

From these plots, the maximum transmittance and minimum light reflectance was attained for M3 coated solar cell as 95 % and 4 %. Also, it is clear that increasing the

coating thickness increases light transmittance by minimizing reflectance up to 288 nm (M3) coated solar cell. Further increase in coating thickness lead to the declined light transmittance and increased reflectance. The AR coating beyond optimal thickness (288 nm) inhibits the light reaching the depletion region (for M4 coated sample), hence a minimum quantity of exciton generation occurs due to maximum light scattering [13, 18].

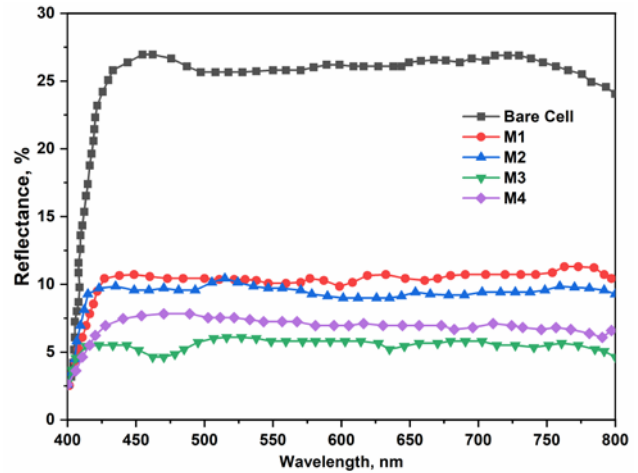


**Fig. 7.** Optical reflectance of various  $\text{MoS}_2$  sputter deposited solar cells

The four probe method helps to examine the electrical resistivity of bare cell and other coated samples that are represented in Fig. 8. The resistivity of bare cell and other coated samples (M1 to M4) were found to be  $8.7 \times 10^{-3} \text{ ohm-cm}$ ,  $5.75 \times 10^{-3} \text{ ohm-cm}$ ,  $4.07 \times 10^{-3} \text{ ohm-cm}$ ,  $2 \times 10^{-3} \text{ ohm-cm}$  and  $3.07 \times 10^{-3} \text{ ohm-cm}$ . From these data, the resistivity decreases up to certain extent (288 nm). The increase in power conversion efficiency (PCE) is mainly because of the existence of Mo and S elements. Beyond that thickness, there is an increase in electrical resistivity due to increased coating thickness [19] and found to be  $3.07 \times 10^{-3} \text{ ohm-cm}$ .

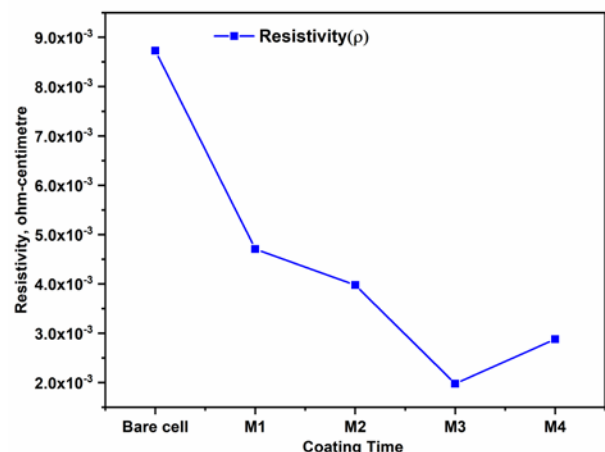


**Fig. 8.** Resistivity of various  $\text{MoS}_2$  sputter deposited solar cells

$\text{MoS}_2$  coated and the uncoated solar cell was analysed under open and controlled working environment. The PCE of various solar cells under open conditions are tabulated in Table 3. I-V values of different  $\text{MoS}_2$  coated samples and the uncoated solar cell are plotted in Fig. 9. Under the open

conditions, the solar cell was placed under direct sunlight and then its performance was analysed. I-V measurement was performed by Keithley I-V source meter and kick start interfacing software. A pyranometer helps to measure the solar radiation at that instant. The solar cell was analysed at 12.00 pm where maximum solar radiation occurs. From Table 3, it is clear that increase in short circuit current ( $I_{sc}$ ) and open circuit voltage ( $V_{oc}$ ) results in increased cell performance. In particular, the M3 coated sample showed maximum solar cell performance of 19.19%. Furthermore, increasing coating thickness lead to decrease in  $V_{oc}$  and  $I_{sc}$ .

The main reason for declined cell performance after 30 minutes of the coating was due to increased coating layer thickness. This in turn inhibits the light transmittance reaching the depletion region.

**Table 3.** I-V measurement of various coated samples at open source environment

Coated samples	Open circuit voltage, V	Short circuit current, mA/cm <sup>2</sup>	Fill factor, %	PCE, %
Bare cell	0.633	31.75	76.30	14.97
M1	0.635	32.52	76.54	15.38
M2	0.648	36.48	77.13	17.11
M3	0.653	39.02	78.11	19.19
M4	0.651	38.69	77.26	17.97

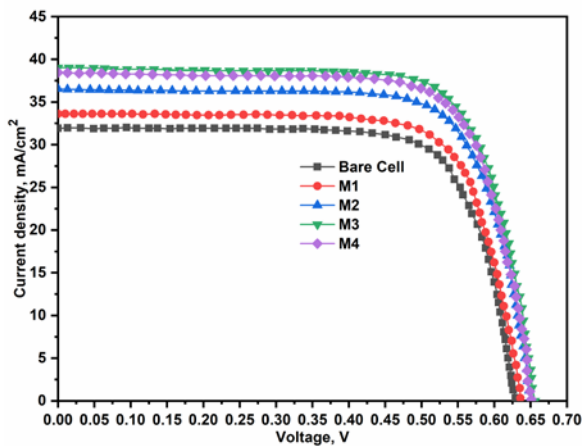


**Fig. 9.** I-V Plot of various MoS<sub>2</sub> sputter deposited solar cells under direct sunlight (open)

In the closed conditions, neodymium lamp acts as a solar simulator and is capable of emitting one sun radiation (1000 W/m<sup>2</sup>). There is a very minimum fluctuation of incident light radiation under controlled light source. The generated PCE,  $I_{sc}$  and  $V_{oc}$  values of bare cell and the coated cell are tabulated in Table 4.

**Table 4.** I-V measurement of various coated samples at closed source environment

Coated samples	Open circuit voltage, V	Short circuit current, mA/cm <sup>2</sup>	Fill factor, %	PCE, %
Bare cell	0.631	33.52	75.12	15.88
M1	0.637	36.52	76.10	17.54
M2	0.654	38.60	77.00	19.42
M3	0.667	40.92	77.79	21.01
M4	0.665	39.58	71.80	20.03

Under the closed condition, there is a constant light illumination which always results in slightly enhanced performance of the solar cell. The uncoated solar cell exhibits  $V_{oc}$  of 0.631 V,  $I_{sc}$  of 33.52 mA/cm<sup>2</sup>, FF of 75.12% and PCE of 15.88%. From experimentation, the 30 minutes coated solar cell (M3) showed maximum solar cell performance with PCE of 19.42%. Increasing coating time increases the efficiency from 15.88 to 19.42%. Further increase in coating thickness leads to a drop in cell performance with a subsequent decrease in  $I_{sc}$  and  $V_{oc}$ [20]. Fig. 10 depicts the I-V characteristic curve of MoS<sub>2</sub> coated and uncoated solar cells under closed operating conditions.

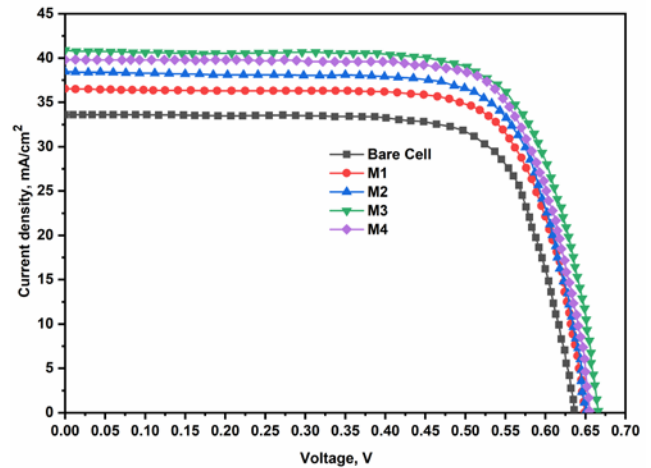


**Fig. 10.** I-V Plot of various MoS<sub>2</sub> sputter deposited solar cells under neodymium illumination (controlled source)

Fig. 11 and Fig. 12 represents the thermal behaviour of uncoated and AR coated solar cells (M1, M2, M3 and M4) under open and controlled operating conditions.

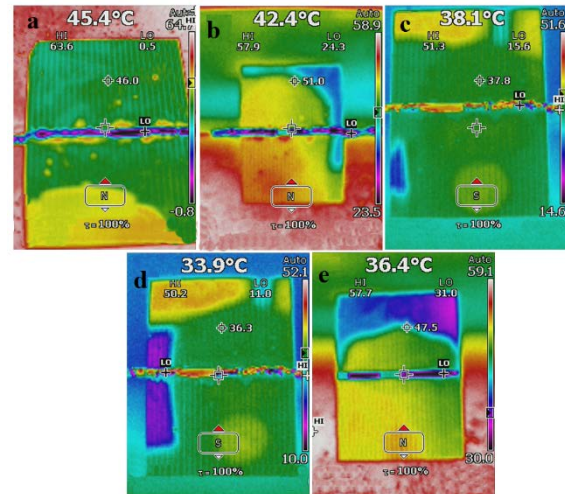


**Fig. 11.** Thermal images: a – uncoated; b – M1; c – M2; d – M3; e – M4 solar cell samples (open source)

Due to constant light illumination in closed source, maximum heat can be experienced by the solar cell than in open atmospheric conditions. The solar cell temperature is inversely proportional to the solar cell performance and directly proportional to electrical resistivity [21, 22]. Thermal images of various solar cell samples under open and closed conditions were captured using I-R fluke

thermal imager. From results, M3 coated solar cell experiences minimum cell temperature, maximum PCE and minimum electrical resistivity.

From various observations, M3 reported open condition working temperature (33.9 °C) and closed condition temperature (49.9 °C).

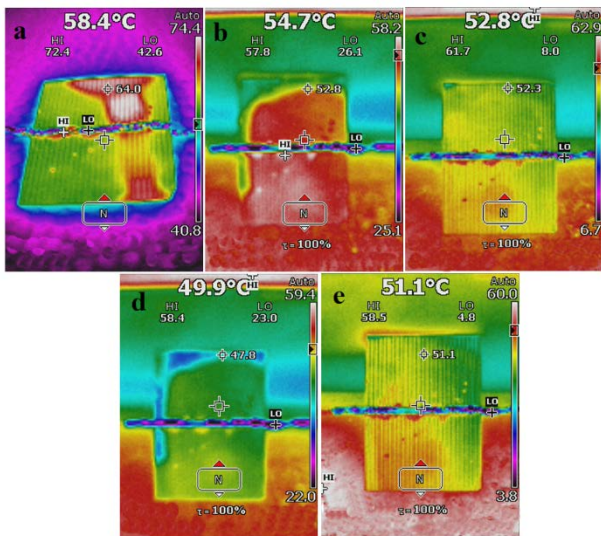


**Fig. 12.** Thermal images: a – uncoated; b – M1; c – M2; d – M3; e – M4 solar cell samples (controlled condition)

Increase in heat flux indirectly indicates reduction in transparency of coated layer and enhanced light scattering. Hence 658 nm thickness of MoS<sub>2</sub> coated solar cell is found to be optimal thickness for attaining maximum cell performance.

#### 4. CONCLUSIONS

From various experimentations, it is observed that transition metal chalcogenide MoS<sub>2</sub> holds antireflective property and hence allows more photons to pass through the surface coated films. Through RF sputter deposition, MoS<sub>2</sub> was coated at various sputter times. The cross sectional thickness of coated layers such as 98 nm, 176 nm, 288 nm and 378 nm were examined through FESEM images. The XRD pattern of synthesised MoS<sub>2</sub> was found to be in accordance with the standard diffraction pattern. The maximum light transmittance and minimum reflectance of 95 % and 4 % are attained for the M3 coated solar cell. Polycrystalline Si solar cell with 30 minutes of MoS<sub>2</sub> (M3) exhibits maximum PCE of 21.01 % (controlled source) and 19.19 % (open source). The M3 coating was found to have optimal thickness with which maximum light transmittance occurs resulting in maximum solar cell performance.

#### REFERENCES

1. Ye, L., Zhang, Y., Zhang, X., Hu, T., Ji, R., Ding, B., Jiang, B. Sol-gel Preparation of SiO<sub>2</sub>/TiO<sub>2</sub>/SiO<sub>2</sub>-TiO<sub>2</sub> Broadband Antireflective Coating for Solar Cell Cover Glass *Solar Energy Materials and Solar Cells* 111 2013: pp. 160 – 164. <https://doi.org/10.1016/j.solmat.2012.12.037>
2. Kaliyannan, G.V., Palanisamy, S.V., Rathanasamy, R., Palanisamy, M., Palaniappan, S.K., Chinnasamy, M. Influence of Ultrathin Gahnite Anti-Reflection Coating on the

- Power Conversion Efficiency of Polycrystalline Silicon Solar Cell *Journal of Materials Science: Materials in Electronics* 31 2020: pp. 2308 – 2319. <https://doi.org/10.1007/s10854-019-02763-2>
3. Kaliyannan, G.V., Palanisamy, S.V., Priyanka, E., Thangavel, S., Sivaraj, S., Rathanasamy, R. Investigation on Sol-Gel based Coatings Application in Energy Sector – A Review *Materials Today: Proceedings* 45 2021: pp. 1138 – 1143. <https://doi.org/10.1016/j.matpr.2020.03.484>
4. Kaliyannan, G.V., Palanisamy, S.V., Rathanasamy, R., Palanisamy, M., Nagarajan, N., Sivaraj, S., Anbupalani, M.S. An Extended Approach on Power Conversion Efficiency Enhancement through Deposition of ZnS-Al<sub>2</sub>S<sub>3</sub> Blends on Silicon Solar Cells *Journal of Electronic Materials* 49 2020: pp. 5937 – 5946. <https://doi.org/10.1007/s11664-020-08361-x>
5. Chen, D. Anti-Reflection (AR) Coatings made by Sol-Gel Processes: A Review *Solar Energy Materials and Solar Cells* 68 2001: pp. 313 – 336. [https://doi.org/10.1016/S0927-0248\(00\)00365-2](https://doi.org/10.1016/S0927-0248(00)00365-2)
6. Dobrzański, L., Szindler, M., Drygala, A., Szindler, M. Silicon Solar Cells with Al<sub>2</sub>O<sub>3</sub> Antireflection Coating *Open Physics* 12 2014: pp. 666 – 670. <https://doi.org/10.2478/s11534-014-0500-9>
7. Scholtz, E., Šutta, P., Calta, P., Novák, P., Solanská, M., Müllerová, J. Investigation of Barium Titanate Thin Films as Simple Antireflection Coatings for Solar Cells *Applied Surface Science* 461 2018: pp. 249 – 254. <https://doi.org/10.1016/j.apsusc.2018.06.226>
8. Sharma, R., Amit, G., Ajit, V. Effect of Single and Double Layer Antireflection Coating to Enhance Photovoltaic Efficiency of Silicon Solar *Journal of Nano- and Electronic Physics* 9 (2) 2017: pp. 02001(1 – 4). [https://doi.org/10.21272/jnep.9\(2\).02001](https://doi.org/10.21272/jnep.9(2).02001)
9. Uzum, A., Kuriyama, M., Kanda, H., Kimura, Y., Tanimoto, K., Fukui, H., Izumi, T., Harada, T., Ito, S. Sprayed and Spin-coated Multilayer Antireflection Coating Films for Nonvacuum Processed Crystalline Silicon Solar Cells *International Journal of Photoenergy* 2017 (1) 2017: pp. 1 – 5. <https://doi.org/10.1155/2017/3436271>
10. Satha, S., Sahu, R., Mun, J., Kim, K. Thermolytic Deposition of MoS<sub>2</sub> Nanolayer for Si Solar Cell Applications *Physica Status Solidi (a)* 217 2020: pp. 1900993 (1 – 7). <https://doi.org/10.1002/pssa.201900993>
11. Patidar, R., Burkitt, D., Hooper, K., Richards, D., Watson, T. Slot-die Coating of Perovskite Solar Cells: An overview *Materials Today Communications* 22 2020: pp. 100808. <https://doi.org/10.1016/j.matcomm.2019.100808>
12. Sukharevska, N., Bederak, D., Goossens, V.M., Momand, J., Duim, H., Dirin, D.N., Kovalenko, M.V., Kooi, B.J., Loi, M.A. Scalable PbS Quantum Dot Solar Cell Production by Blade Coating from Stable Inks *ACS Applied Materials & Interface* 13 2021: pp. 5195 – 5207. <https://doi.org/10.1021/acsami.0c18204>
13. Kaliyannan, G.V., Palanisamy, S.V., Palanisamy, M., Subramanian, M., Paramasivam, P., Rathanasamy, R. Development of Sol-gel Derived Gahnite Anti-Reflection Coating for Augmenting the Power Conversion Efficiency of Polycrystalline Silicon Solar Cells *Materials Science Poland* 37 2019: pp. 465 – 472. <https://doi.org/10.2478/msp-2019-0066>

14. **Ayyar, M., Mani, M.P., Jaganathan, S.K., Rathanasamy, R.** Preparation, Characterization and Blood Compatibility Assessment of a Novel Electrospun Nanocomposite Comprising Polyurethane and Ayurvedic-Indhulekha Oil for Tissue Engineering Applications *Biomedical Engineering/Biomedizinische Technik* 63 2018: pp. 245 – 253.  
<https://doi.org/10.1515/bmt-2017-0022>
15. **Jaganathan, S.K., Mani, M.P., Ayyar, M., Rathanasamy, R.** Biomimetic Electrospun Polyurethane Matrix Composites with Tailor Made Properties for Bone Tissue Engineering Scaffolds *Polymer Testing* 78 2019: pp. 105955.  
<https://doi.org/10.1016/j.polymertesting.2019.105955>
16. **Tombak, A., Kilicoglu, T., Ocak, Y.S.** Solar Cells Fabricated by Spray Pyrolysis Deposited  $\text{Cu}_2\text{CdSnS}_4$  Thin Films *Renewable Energy* 146 2020: pp. 1465 – 1470.  
<https://doi.org/10.1016/j.renene.2019.07.057>
17. **Somrani, N., Maaloul, A., Saidi, H., Stafford, L., Gaidi, M.** Microstructural and Optical Properties Tuning of Bifeo 3 Thin Films Elaborated by Magnetron Sputtering *Journal of Materials Science: Materials in Electronics* 26 2015: pp. 3316 – 3323.  
<https://doi.org/10.1007/s10854-015-2833-6>
18. **Hou, Q., Meng, F., Sun, J.** Electrical and Optical Properties of Al-Doped ZnO And  $\text{ZnAl}_2\text{O}_4$  Films Prepared by Atomic Layer Deposition *Nanoscale Research Letters* 8 2013: pp. 1 – 8.  
<https://doi.org/10.1186/1556-276X-8-144>
19. **Dixit, H., Tandon, N., Cottenier, S., Saniz, R., Lamoen, D., Partoens, B.** First-Principles Study of Possible Shallow Donors in  $\text{ZnAl}_2\text{O}_4$  Spinel *Physical Review B* 87 2013: pp. 174101.  
<https://doi.org/10.1103/PhysRevB.87.174101>
20. **Chanta, E., Bhoomanee, C., Gardchareon, A., Wongratanaphisan, D., Phadungdhithidhada, S., Choopun, S.** Development of Anti-Reflection Coating Layer for Efficiency Enhancement of ZnO Dye-Sensitized Solar Cells *Journal of Nanoscience and Nanotechnology* 15 2015: pp. 7136 – 7140.  
<https://doi.org/10.1166/jnn.2015.10538>
21. **Dubey, S., Sarvaiya, J.N., Seshadri, B.** Temperature Dependent Photovoltaic (PV) Efficiency and its Effect on PV Production in the World—A Review *Energy Procedia* 33 2013: pp. 311 – 321.  
<https://doi.org/10.1016/j.egypro.2013.05.072>
22. **Radziemska, E.** The Effect of Temperature on the Power Drop in Crystalline Silicon Solar Cells *Renewable Energy* 28 2003: pp. 1 – 12.  
[https://doi.org/10.1016/S0960-1481\(02\)00015-0](https://doi.org/10.1016/S0960-1481(02)00015-0)



© Shanmugam et al. 2022 Open Access This article is distributed under the terms of the Creative Commons Attribution 4.0 International License (<http://creativecommons.org/licenses/by/4.0/>), which permits unrestricted use, distribution, and reproduction in any medium, provided you give appropriate credit to the original author(s) and the source, provide a link to the Creative Commons license, and indicate if changes were made.